JOURNAL OF GEOPHYSICAL RESEARCH, VOL. 99, NO. A4, PAGES 6011–6025, APRIL 1, 1994

Identification of low-frequency fluctuations in the terrestrial magnetosheath

P. Song
High Altitude Observatory, National Center for Atmospheric Research, Boulder, Colorado

C. T. Russell
Institute of Geophysics and Planetary Physics, University of California, Los Angeles

S. P. Gary
Los Alamos National Laboratory, Los Alamos, New Mexico

Abstract. On the basis of MHD theory we develop a scheme for distinguishing among the four low-frequency modes which may propagate in a high-β anisotropic plasma such as the magnetosheath: the fast and slow magnetosonic, the Alfvén, and mirror modes. We use four parameters: the ratio of transverse to compressional powers in the magnetic field, the ratio of the wave powers in the thermal pressure and in the magnetic field, the ratio of the perturbations in the thermal and magnetic pressures, and the ratio of the wave powers in the velocity and in the magnetic field. In the test case of an Active Magnetospheric Particle Tracer Explorers/Ion Release Module (AMPTE/IRM) magnetosheath pass near the Sun-Earth line downstream of a quasi-perpendicular shock, the four modes can be clearly distinguished both spatially and spectrally. Near the bow shock, the waves are Alfvénic in a large frequency range, 1 to 100 mHz. In the middle and inner magnetosheath, the waves below 10 mHz are Alfvénic. The fast mode waves occur in the higher-frequency end of the enhanced spectrum, 80 mHz for the middle magnetosheath and 55 mHz for the inner sheath. The wave enhancement in the intermediate frequencies is slow modes in the inner sheath and mirror modes in the middle sheath. This confirms the earlier report of the existence of the slow mode waves near the magnetopause. These slow waves provide evidence that the magnetopause is an active source of the waves in the sheath. We also show that the measured frequency of a wave is close to an invariant if the magnetosheath flow is in a steady state. Therefore changes in the frequencies of enhanced waves indicate emergence, or damping, or mode conversion of the waves.

Introduction

The dayside magnetosheath provides a natural laboratory to study the interaction between a subsonic magnetized plasma flow and a blunt body, the magnetopause. However, because the solar wind is supersonic and there exists a bow shock, the magnetosheath fills with waves. Some of these are the products of interaction of the solar wind with the bow shock, some are related to the final interaction with the magnetopause, and some are the results of the coupling between the waves of the first two sources. For example, particles accelerated at the shock can generate waves in the foreshock which are convected into the magnetosheath, and the anisotropic heating at the bow shock can destabilize waves in the sheath flow. Near the bow shock, ion cyclotron waves and mirror waves have been observed downstream of quasi-perpendicular shocks [*Sckopke et al.*, 1990; *Lacombe et al.*, 1992] and theoretically investigated [*Brinca et al.*, 1990; *Price et al.*, 1986, *Lee et al.*, 1988]. Near the magnetopause, the change from low-frequency compressional waves [*Kaufmann et al.*, 1970; *Tsurutani et al.*, 1982; *Russell et al.*, 1987] to high-frequency transverse waves [*Cummings and Coleman,* 1968; *Neugebauer et al.*, 1974; *Fairfield,* 1976; *Rezeau et al.*, 1989] has also been reported and studied [*Song et al.*, 1990a, 1993; *Anderson et al.*, 1991, 1994; *Takahashi et al.*, 1991; *Gary et al.*, 1993]. This change is due to the interaction of the plasma with the magnetopause. A physically similar change also occurs in the region slightly upstream of the magnetopause at lower frequencies [*Song et al.*, 1990b, 1992a, b; *Lee et*

Copyright 1994 by the American Geophysical Union.

Paper number 93JA03300.
0148-0227/94/93JA-03300$05.00

al., 1991; *Southwood and Kivelson*, 1992; *Hubert*, 1994; *Omidi and Winske*, 1992; *Omidi et al.*, 1994]. However, the waves in the magnetosheath are still poorly understood. Identification of the various wave modes is the first step toward understanding the physical processes in the magnetosheath.

In this paper we concentrate on mode identification of the low-frequency fluctuations, which have periods much longer than the ion gyroperiod. Because such low-frequency waves contain significant energy in the context of the solar wind-magnetosphere interaction, they have received much attention. Observationally, *Engebretson et al.* [1991] provided the morphology of these waves and emphasized their coupling to the waves in magnetosphere. They found that the waves in the Pc 3-4 range, with periods from 10 s to 2.5 min, are controlled by the shock geometry; i.e., the interplanetary magnetic field (IMF) is either perpendicular or parallel to the bow shock normal. The waves downstream of quasi-parallel shocks are much stronger and more turbulent than those downstream of quasi-perpendicular shocks. *Lin et al.* [1991a] introduced a disturbance parameter to characterize the degree of turbulence of the waves, and *Lin et al.* [1991b] studied the energy fluxes in these waves. *Gleaves and Southwood* [1991] concentrated on the mode identification comparing the measurements from two separated spacecraft with MHD disperson relations. An important feature of their studies is that they discussed the Doppler effects on propagating waves. *Lacombe et al.* [1992] and *Hubert et al.* [1989a, b] incorporated the results from theoretical calculations with observations to understand the nature of the waves. They have drawn attention to the ratios of the perturbations which have inspired the present study. While much of the theoretical research has focused on the mirror instability [*Price et al.*, 1986; *Lee et al.*, 1988; *McKean et al.*, 1992; *Gary*, 1992; *Southwood and Kivelson*, 1994], *Gary and Winske* [1992] parameterized the transport ratios for each wave mode, which work provides the basis for this study.

The magnetosheath β, the ratio between the thermal pressure and magnetic pressure, is usually greater than unity in most regions other than the region very close to the subsolar magnetopause. This high-β nature indicates that the classical wave analysis methods developed primarily to utilize magnetic field measurements are not sufficient. In a high-β plasma, the electromagnetic force, $\mathbf{JxB}$, becomes weaker than the plasma thermal force ∇p, and dynamical forces, $\nabla \rho v^2$, for example, where $\mathbf{J}, \mathbf{B}, p, \rho$, and v are the electric current density, magnetic field, thermal pressure, plasma density, and velocity. For high-β waves, plasma parameters become as important as magnetic parameters, so that the magnetic field is weak and easily distorted, making it easier for the fluctuations to reach a nonlinear stage. The magnetosheath conditions also change over a wide parameter range depending on the solar wind conditions, shock geometry, and location within the magnetosheath. For example, the temperature anisotropy may be a strong function of shock geometry. Another difficulty in analyzing the magnetosheath waves is that no simple organizing coordinate system is available. Because the IMF may change suddenly during a magnetosheath pass, field-aligned coordinates may be highly noninertial at these changes. Furthermore, the running average used to determine field-aligned coordinates may artificially introduce waves at the field rotations and these waves can propagate into both sides of a field rotation.

Despite all these problems, the most difficult issue concerning the study of these waves is to determine the Doppler shift, the difference between the frequency measured in the spacecraft frame and that in the plasma frame. Since most theories provide the frequency in the plasma frame, without knowing the Doppler shift any comparison of observation with theory may be inappropriate. The Doppler shift can be easily resolved if the flow velocity is either much less or much greater than the phase velocity of the wave. Either condition requires the knowledge of the wave mode. However, in the magnetosheath, there exist a variety of modes and the waves may propagate either upstream or downstream. The phase velocity of some modes may be comparable with the flow velocity in some regions, bearing in mind that the flow velocity continuously changes from the bow shock to the dayside magnetopause. Recent observation of slow mode waves near the dayside magnetopause [*Song et al.*, 1992a, b; *Hubert*, 1994; *Omidi et al.*, 1994] has indicated the importance of the Doppler shift in mode identification.

A particular problem in the magnetosheath is distinguishing the fluctuations associated with the mirror instability from the slow mode wave. Both fluctuations are compressible and exhibit density fluctuations of 180° out of phase with the magnetic field strength fluctuations. Because the slow mode is heavily damped in linear kinetic theory, some previous studies have assumed all the compressional waves with the thermal pressure and magnetic pressure out of phase to be mirror modes. However, the mirror modes could play a minor role in the magnetosheath field and velocity reconfiguration because in the saturation stage they produce only a weak velocity perturbation in the plasma frame. *Song et al.* [1992b] used measurements from two separated spacecraft to resolve the difference between slow modes and mirror modes and proved the existence of the slow mode waves. The significance of this finding is that the magnetopause is not simply a passive recipient of the sheath waves, but must be an active source of these waves.

In this paper, we first (section 2) introduce and discuss, based on MHD theory, the four parameters to be used in identifying four wave modes. In addition, we show, in section 3, that the frequency observed in the spacecraft frame is close to an invariant as the flow changes its magnitude and direction through the magnetosheath. Next, in section 4, we test the method in one AMPTE/IRM magnetosheath pass. We discuss briefly the nonlinear effects concerning the slow mode wave in section 5.

Theoretical Scheme

The properties of each mode discussed in this section are based on MHD theory. The results of the study are also consistent qualitatively with those when kinetic effects are included [e.g., *Gary and Winske*, 1992]. We give the qualitative distinctions between the modes but do not imply that the MHD theory precisely describes all of the wave properties. In classical isotropic MHD there are three propagating wave modes, the fast, intermediate and slow modes. In addition, there is a nonpropagating mode, the entropy mode. The fast and slow modes are compressional, the former with magnetic pressure and thermal pressure varying in phase and the latter 180° out of phase. The intermediate mode is incompressible. Since kinetic effects cause a switch in the order between the phase velocities of the slow and intermediate modes in high-β plasma, we refer to the incompressible mode as an Alfvén mode in this paper. In the more general case of anisotropic MHD, there is also the so-called mirror mode, an instability which arises in the slow magnetosonic branch of the MHD dispersion relation when a finite temperature anisotropy is included. The mirror instability is a purely growing mode with a near-zero real frequency, $\omega_r^2 \ll (v_{th||}k_{||})^2$ and $\omega_r^2 \ll (C_A k)^2$, where $k_{||}, k, v_{th||}$ and C_A are the parallel component and magnitude of the wave vector, the parallel thermal velocity, and the Alfvén velocity. The kinetic treatment suggests that it is more appropriate to consider the mirror mode as the entropy mode in classical MHD [e.g., *Krauss-Varban et al.*, 1994] and not MHD slow modes [*Southwood and Kivelson*, 1993]. In the saturation stage, the mirror mode instability forms a series of magnetic cavities [*Hasegawa*, 1975]. When these magnetic cavities convect with the magnetosheath flow, due to the Doppler shift, they appear to be waves. These mirror waves have some characteristics similar to the slow magnetosonic waves and have sometimes been confused with the slow magnetosonic waves in observations.

In principle, to identify four wave modes, at least four independent parameters are needed if only one condition is used for each parameter. In the following we discuss the four parameters which are used in our study. We have examined and tested various combinations of different parameters and found that some parameters are very sensitive to the wave amplitude; i.e., when the amplitude is large, they behave irregularly. Some other parameters, such as the magnetic potential, are not conveniently obtained from observations, although they are easily treated theoretically. Other parameters, such as the Alfvén velocity, require accurate intercalibration among different instruments.

Transverse ratio. We define this ratio as the transverse wave power of the magnetic field versus the compressional power or

$$T = (\delta\mathbf{B}\cdot\delta\mathbf{B} - \delta B_{||}^2)/\delta B_{||}^2 \tag{1}$$

where $\delta\mathbf{B}$ is the perturbed magnetic field vector and $\delta B_{||}$ is the perturbed component of the magnetic field parallel to $\mathbf{B}_0$, the background field. This parameter has been widely used in magnetospheric wave studies and is easy to obtain observationally over a wide range of frequencies. For the Alfvén mode, this parameter is much greater than unity. For the two compressional modes, its value is less clear. Because the two compressional modes obey coplanarity, from $\nabla\cdot\mathbf{B} = 0$ we have

$$-\frac{\delta B_z}{\delta B_x} = \frac{k_x}{k_z} = \tan\theta \tag{2}$$

Here we have assumed the xz plane is the coplanar plane which contains the background field and wave vector, and the background field is along z. The transverse ratio is determined by the propagation angle θ for the two compressional modes. If we define the transverse waves as satisfying $\delta B_x > \delta B_z$, the two compressional modes are transverse when they propagate quasi-parallel to the background field with a transverse ratio greater than 1. When such modes propagate in a quasi-parallel direction, they are difficult to distinguish from the Alfvén mode and other noise by only the transverse ratio. Because the mirror instability has a wave vector relatively perpendicular to the background field, the mirror modes are predominantly compressional.

Compressional ratio. We define the compressional ratio as the ratio of the wave power in the plasma thermal pressure to that in the magnetic field, or

$$C = \frac{\delta P_i^2}{P_{i0}^2}\frac{B_0^2}{\delta\mathbf{B}\cdot\delta\mathbf{B}} \tag{3}$$

where $\delta P_i, P_{io}$, and B_0 are the perturbed thermal pressure and the average thermal pressure and field strength. From the MHD dispersion relation, it can be shown (see appendix A) that in a high-β plasma for nearly parallel propagating waves, the compressional ratio goes to infinity for fast magnetosonic modes and goes to zero for slow magnetosonic modes. Therefore the compressional ratio of quasi-parallel propagating fast magnetosonic waves should be greater than unity and for slow magnetosonic waves it should be smaller than unity. Physically, this is because in a high-β plasma, the fast mode is similar to sound waves and carries most compression. In MHD, the Alfvén and slow magnetosonic modes are degenerate in a high-β plasma at quasi-parallel propagation and hence indistinguishable. In the following discussion, we refer to them as Alfvénic or Alfvén-like waves. Thus at high β, the fast magnetosonic mode for quasi-parallel propagation may be uniquely identified by its two properties $T \gg 1$ and $C > 1$. Note that the differences between quasi-perpendicular Alfvén mode and quasi-parallel slow magnetosonic modes remain unresolved in our scheme.

Partition ratio. We define the partition ratio as the wave perturbation in the plasma thermal pressure versus that in the magnetic pressure, or

$$P = \frac{\delta P_i}{P_{io}}\frac{P_{Bo}}{\delta P_B} \tag{4}$$

where δP_B and P_{Bo} are the perturbed and background magnetic pressure, $B^2/2\mu_0$. From the MHD dispersion relation for the two compressional modes we have

$$P = \frac{\gamma}{2}\left(1 - \frac{c_s^2 \cos^2\theta}{v_{ph}^2}\right)^{-1} \quad (5)$$

where γ, c_s, and v_{ph} are the polytropic index, sound speed, and phase speed. For slow (fast) magnetosonic modes at quasi-perpendicular propagation in a high-β plasma, $c_s \cos\theta$ is greater (smaller) than the phase velocity, so that P is negative (positive). This identifier has been used in most observations to distinguish fast from slow magnetosonic and mirror modes. For Alfvén modes, this parameter has not proven useful because it is the ratio of two small values and is affected by noise. Here we point out that this parameter does not resolve the differences between slow magnetosonic modes and mirror modes. This parameter is similar to the compressibility of *Lacombe et al.* [1992] and the parallel compressibility of *Gary and Winske* [1992]. We choose this new ratio because in practice the coherence between the thermal pressure and magnetic pressure is higher than that between the density and field strength; i.e., the thermal pressure is less sensitive to thermal noise than the density.

Doppler ratio. We defined the Doppler ratio as the perturbation power in the velocity versus that in the magnetic field, or

$$D = \frac{\delta\mathbf{v}\cdot\delta\mathbf{v}}{v_0^2}\,\frac{B_0^2}{\delta\mathbf{B}\cdot\delta\mathbf{B}} \quad (6)$$

where $\delta\mathbf{v}$ and v_0 are the perturbed velocity and magnitude of the background flow velocity. Note that this parameter is not the same as the Alfvén ratio for which the velocity perturbations are normalized by the Alfvén velocity [*Matthaeus and Goldstein*, 1982a; *Gary and Winske*, 1992]. It carries the information of the flow, which is not carried in the Alfvén ratio. We use it to distinguish mirror modes from slow magnetosonic modes. In general, slow magnetosonic waves have perturbations in both the velocity and magnetic field, but mirror mode fluctuations do not produce significant velocity perturbations. Therefore if the flow is sub-Alfvénic, the Doppler ratio is greater than unity for quasi-perpendicular slow magnetosonic modes and should be much smaller than one for mirror modes, as shown in the appendix A.

The scheme of mode identification described above is summarized in Figure 1. Although it is based on MHD linear theory, it is also qualitatively consistent with the results from kinetic theory under the similar conditions, (e.g., Table 2b of *Gary and Winske* [1992]). The perturbations utilized are for a single wave frequency and a single wavenumber. Because Fourier analysis in the time domain is easy to realize, the identification of the wave modes can be performed in the frequency domain by replacing a perturbation with a Fourier spectrum.

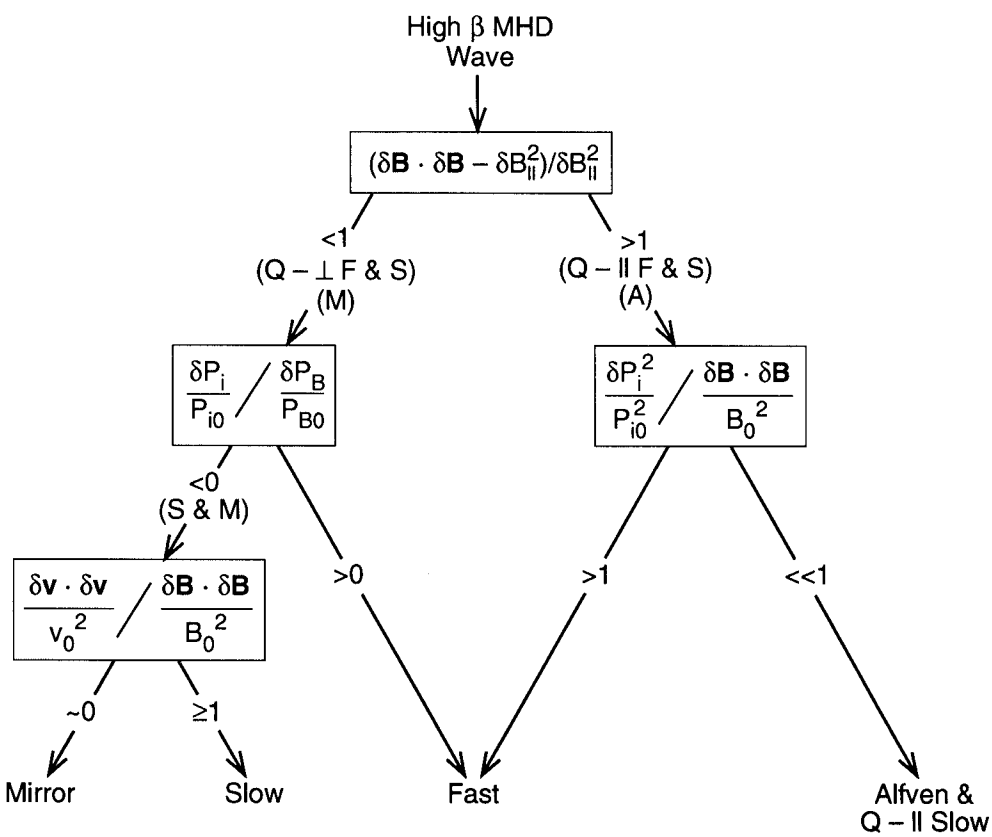

Figure 1. Summary of the theoretical scheme of the MHD wave mode identification. F, S, A, and M denote the fast and slow magnetosonic, Alfvén, and mirror modes, respectively. $Q-\perp$ and $Q-\parallel$ denote quasi-perpendicular and quasi-parallel propagation, respectively.

The assumption here is that a single wave mode is dominant at a single frequency with a single wavenumber.

In theory, all of the physical quantities are equally accurate and therefore the scheme should be parallel among them. In reality, each quantity is measured by a particular technique. They have different uncertainties. A parallel scheme would overemphasize the importance of quantities with greater uncertainties. Our tree-root type scheme is designed according to the accuracy of the measurements to avoid this effect. Namely, if any inconsistency occurs in the mode identification, the higher ratio in Figure 1 overrules the lower one. As there are differences between MHD and kinetic theories, the results based on kinetic theory while using a parallel scheme, namely minimizing the number of inconsistencies in comparison theory with observation, are different from those using the scheme described in this paper. We add some discussion in appendix B on the parallel kinetic scheme.

Frequency Invariant

Because both the plasma and field parameters change through the magnetosheath, the wave parameters also change. The wavelength may change as the plasma compresses (in the dayside) or expands (away from the subsolar point). The propagation angle will also change when the field undergoes reconfiguration from an arbitrary direction in the IMF to tangent to the magnetopause. In general, the interaction of the waves with inhomogeneous medium is very difficult to describe [*Dewar*, 1970; *Barnes*, 1992]. Is anything conserved in the processes? Fortunately, since the inhomogeneity is the result of solar wind-magnetosphere interaction, to lowest order, i.e., in a steady state, it is time independent in the frame at rest with respect to the Earth. The following discussion shows that in a steady state the frequency observed in the Earth frame is conserved and that the frequency observed in the spacecraft frame is close to a constant. This is not necessarily true in other frames.

A variable, such as the density or magnetic field, can be written as $Q(\mathbf{r},t) = Q_0(\mathbf{r}) + Q_1(\mathbf{r},t)$ in the Earth's frame, where $\mathbf{r}$ is the location vector, Q_0 is the steady state component of the quantity, and Q_1 is the perturbed component associated with waves. If we assume that the perturbed variables are small compared with the steady state variables, and that the wavelength is much smaller than the magnetosheath thickness, the time dependent part of Q_1 can be Fourier decomposed [*Barnes*, 1992]. Therefore the frequency ω' in an inertial reference frame which is steady to the flow (e.g., that of Earth) is independent of location and hence is a constant of the motion, or an invariant. It is obvious that the first-order variables satisfy locally the MHD wave equations. Note here the Alfvén velocity, the sound velocity and the propagation angle are functions of location, in other frames, since Q_0 is a function of t and the Fourier decomposition does not apply.

From the nonrelativistic phase conservation, we have

$$\omega' = \omega_{sc} + \mathbf{k}\cdot\mathbf{v}_{sc} = \omega + \mathbf{k}\cdot\mathbf{v}_0 = \mathbf{k}\cdot(\mathbf{v}_{ph} + \mathbf{v}_0) \quad (7)$$

where ω_{sc} is the frequency measured in the spacecraft frame, ω is the frequency as it would be measured in the noninertial frame of the plasma, and $\mathbf{v}_{sc}$ is the velocity of the spacecraft relative to the Earth frame. Here the apparent velocity of the wave as measured in the (inertial) frame of the Earth is the phase velocity v_{ph} plus convection velocity $\mathbf{k}\cdot\mathbf{v}_0/k$. If the apparent velocity is much greater than the spacecraft velocity, then it follows that $\omega_{sc} \approx \omega'$. The spacecraft speed is about 2 km/s in the dayside magnetosheath. For most waves in the magnetosheath, their apparent velocity ranges from a few tens of kilometers per second for quasi-standing slow waves, to about 100 km/s (i.e., the Alfvén speed and sound speed) for the MHD modes. Therefore the frequency for a particular wave measured by a spacecraft in the magnetosheath is close to an invariant if the spacecraft remains on the same streamline and the sheath plasma conditions are relatively steady state. Note that the frequency in the plasma frame, ω, in general changes with location.

In the steady state magnetosheath, changes in the measured frequencies along a streamline must be caused by growth or encountering a new wave, damping of an existing wave, or a wave mode conversion. This invariant eliminates the possibility of the waves with different frequencies observed in different places to be the same but simply with a change in the Doppler shift and provides the possibility to compare the spectra measured in different regions on the same pass if the solar wind and IMF remain unchanged. The changes in the upstream condition will have two effects. First, it breaks down the steady state assumption. To establish a new steady state, it may take a few Alfvén or sonic transient times, about 2 $\sim$ 5 min. Second, the wave properties may change. For example, if the shock geometry changes due to an IMF change, the waves in the magnetosheath before and after the IMF change may be radically different.

Note that the frequency invariant applies to each individual streamline and it may not be the same for different streamlines. Because a spacecraft trajectory may be very different from a streamline, for example, in the flank, changes in frequency may also be caused by sampling different streamlines. Therefore the sufficient condition for the measured frequency to be invariant is either that the spacecraft orbit is near the subsolar region or that the frequency of the wave is not a strong function of the distance from the Sun-Earth line.

Data Analysis

To identify the wave modes using our scheme, we need three-dimensional plasma and magnetic field measurements. Two-dimensional plasma measurements may be applicable in some cases. The frequency range is limited by the data resolution and the interval a spacecraft spends in a wave region. If the data resolution is higher than the ion gyrofrequencies, the Doppler shift

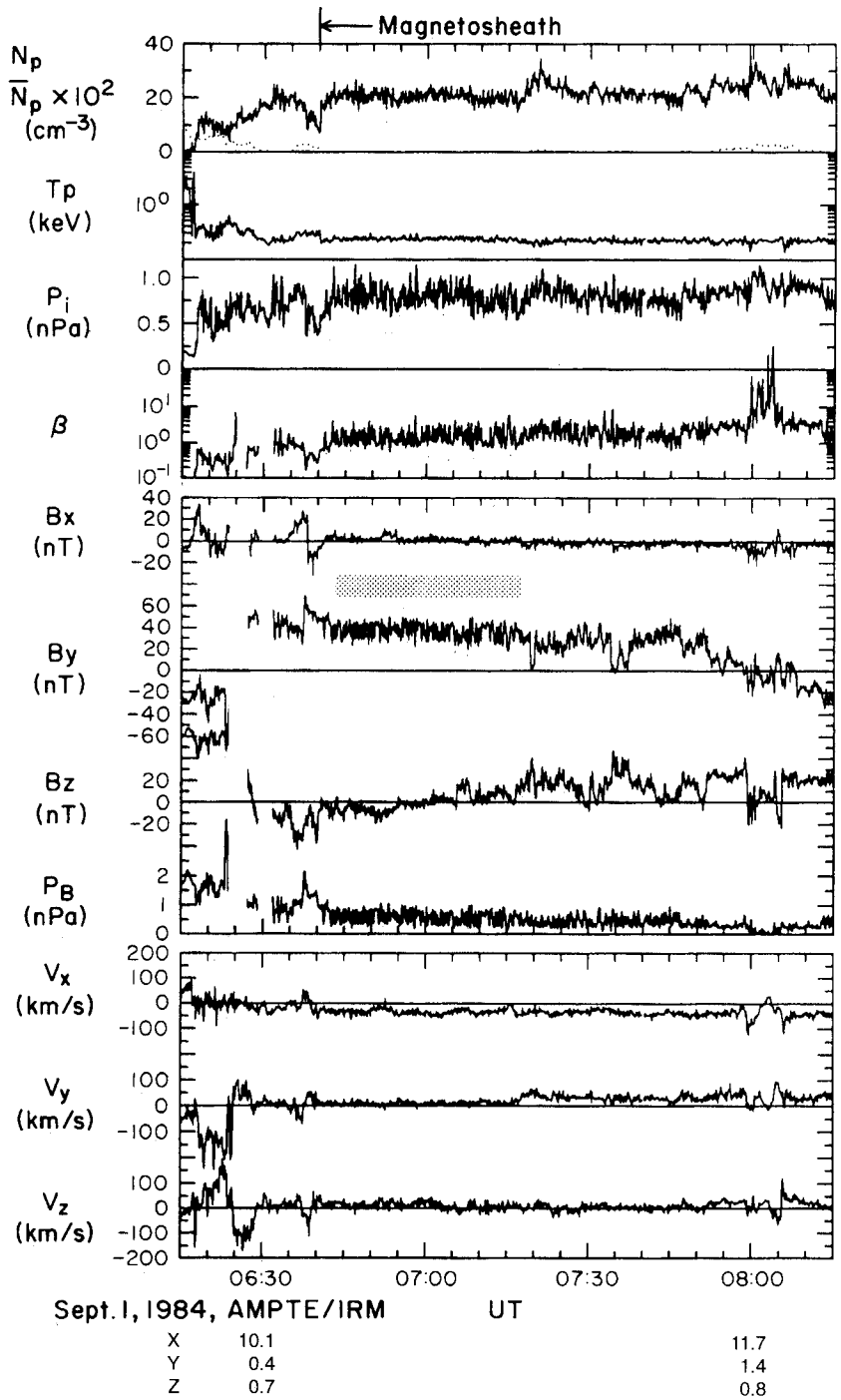

Figure 2. A magnetosheath pass by AMPTE/IRM on September 1, 1984. The data from the top to the bottom are the proton density (solid line) and energetic proton density (dotted line), ion temperature, ion thermal pressures, plasma β, three components of the magnetic field in GSE coordinates, magnetic pressure, and three components of the ion velocity. The data have a time resolution of 5 s. The magnetopause is at about 0640 UT and the bow shock about 1014 UT. The three shaded bars in the middle panel indicate the three time intervals used to test the method. The location of the spacecraft, in R_E GSE, is provided at the bottom.

may need to be taken into account for the applicability of the MHD theory.

To test the theoretical scheme, we have arbitrarily chosen an AMPTE/IRM magnetosheath pass, actually the first pass in the mission for which both plasma and field data are available. This outbound pass occurred near the Sun-Earth line from (10.1, 0.5, 0.7) R_E at 0640 UT to (13.6, 2.7, 0.8) R_E GSE at 1014 UT as shown in Figure 2. The interplanetary magnetic field measurements are available until 0700 UT from ISEE 2, not shown, indicating IRM was downstream of a quasi-perpendicular bow shock. The most striking

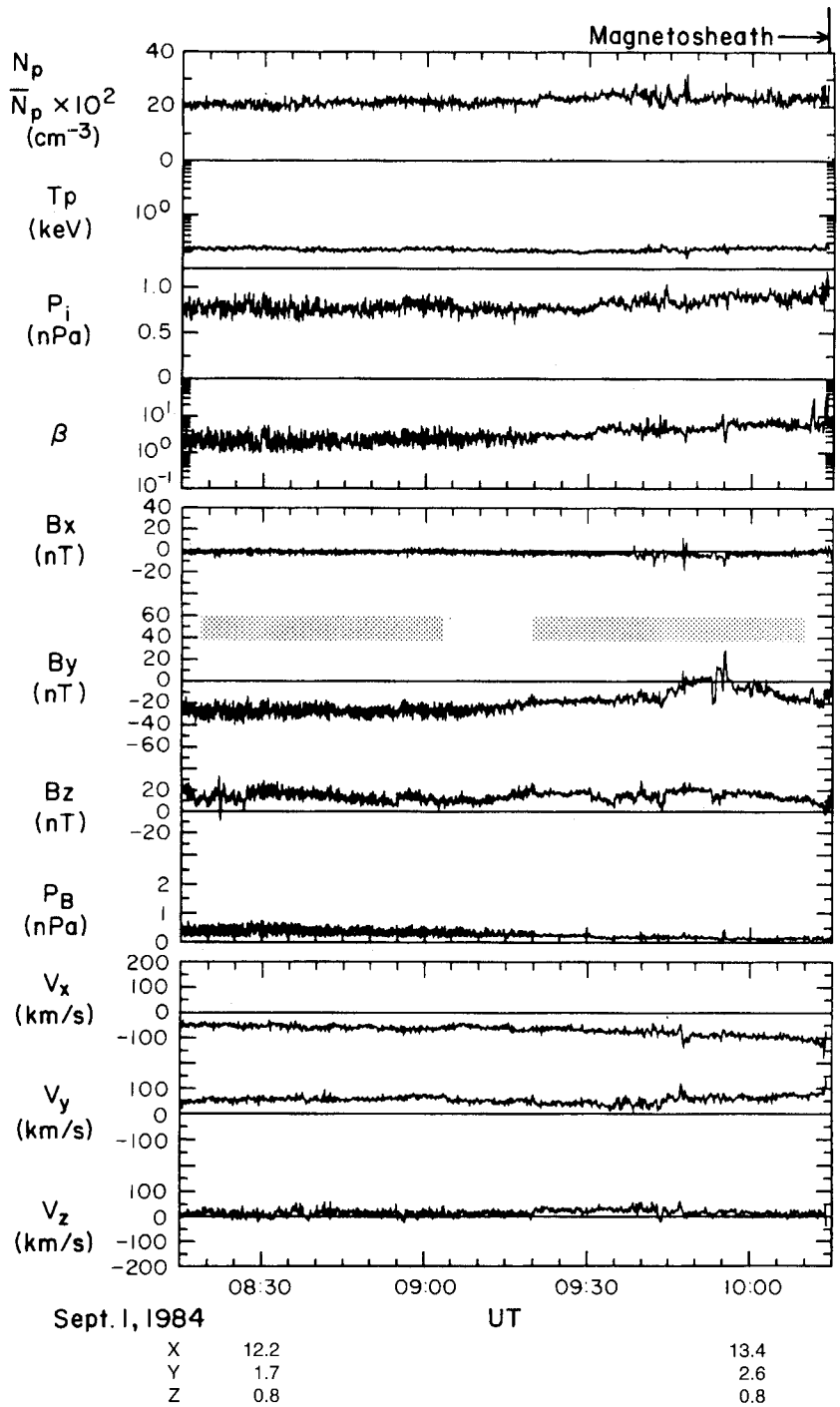

Figure 2. (continued)

wave is the compressional wave with a relatively high frequency. It is not too difficult to see the amplitude of the wave decreases while the frequency increases as the spacecraft moves from the inner sheath to the middle sheath. Although in principle the method described in section 2 can be performed in a dynamic fashion, we chose three time intervals, as indicated by the shaded bars in the middle panels, to test it. The averages of the parameters for each interval are given in Table 1. We Fourier analyze the quantities of $\mathbf{B}, \mathbf{v}, P_i$, and P_B. Here we recall $\delta\mathbf{B} \cdot \delta\mathbf{B} = \delta B_x^2 + \delta B_y^2 + \delta B_z^2, \delta B_\perp^2 = \delta B_x^2 + \delta B_y^2 + \delta B_z^2 - \delta B^2$, and $\delta B_\parallel^2 = \delta B^2$. We use the averages from the same time intervals to normalize the Fourier spectra. The phase relation between the magnetic and thermal pressures is obtained from the cross correlation between the two quantities in the frequency domain. In phase (out of phase) is when the cross correlation is positive (negative).

The Fourier spectra for the interval near the magnetopause are shown in Figure 3. Note that the ratios discussed in section 2, except the partition ratio, are the difference between the two relevant quantities in a logarithmic scale plot. For example, whether the transverse ratio is greater or smaller than 1 becomes a matter of

Table 1. Averages in Each Region of September 1, 1984, IRM Pass

UT	B_0, nT	V_0, km/s	n_0, cm^{-3}	P_{io}, nPa	P_{B_0}, nPa	C_A, km/s
0642 ~ 0718	(1.6, 36.8, 0.3) 37.8	(-32.4, 11.2, 12.0) 40.2	20.4	0.79	0.59	180.6
0816 ~ 0908	(-1.3, -26.8, 13.6) 30.5	(-55.9, 58.3, 13.7) 83.2	21.3	0.78	0.38	142.7
0920 ~ 1010	(-3.0, -10.8, 16.0) 21.6	(-79.3, 52.9, 21.7) 99.8	23.5	0.84	0.19	96.1

whether the spectrum of $\delta B_\perp$ is higher or lower than that of $\delta B_\parallel$. A reminder here is that the unit of a spectrum is the square of the perturbed quantity divided by the frequency. Most significant wave enhancements are between 0.01 and 0.06 Hz and are compressional. The wave below 0.01 Hz is transverse, as are the enhanced fluctuations near 0.08 Hz. The partition ratio is plotted as the bars in the lower part of Figure 3b. Open bars indicate the ratio is negative and shaded bars positive. Of the compressional enhancements, the peak near 0.055 Hz has the magnetic and thermal pressures in phase (see the shaded bar in Figure 3b) and hence is the fast magnetosonic mode. The three lower-frequency peaks are either slow magnetosonic or mirror modes because their magnetic and thermal pressures are out of phase. The compressional ratio is much less than 1 for the low-frequency transverse waves, and thus they are Alfvén-like modes. The high-frequency transverse waves have a compressional ratio close to 1 and are likely to be fast modes. In Figure 3c, the difference between the thick solid line and dashed line gives the square of the Alfvén Mach number v_0/C_A; when the dashed line is lower, the Alfvén Mach number is less than 1. The Doppler ratio is greater than 1 for the three low-frequency compressional peaks, confirming they are slow magnetosonic modes and not mirror modes.

Figure 4 shows the Fourier spectra for the interval in the middle of the magnetosheath. The most significant wave enhancements are still compressional but are at slightly higher frequencies, from 0.04 Hz to 0.08 Hz, compared with the waves in the inner magnetosheath. The compressional fluctuation between 0.04 Hz and 0.07 Hz are mirror modes because of a negative partition ratio and small Doppler ratio. The low frequencies are still dominated by the transverse waves, which is the same condition as in the inner magnetosheath. These transverse waves are Alfvén-like. The compressional peak near 0.08 Hz is the fast magnetosonic mode because of the positive partition ratio.

In the following demonstration, we show how to use the frequency invariant for understanding the evolution of the waves in the magnetosheath by assuming that the frequency of mirror modes remains the same during this IRM pass and that the difference in the frequency on a plane perpendicular to the Sun-Earth line is small near the subsolar region. The second assumption may be relatively easy to satisfy. The accuracy of the first assumption may need further investigation because the IMF may have changed its direction as the spacecraft goes from the inner to the middle sheath. However, most likely the shock geometry remains quasi-perpendicular in both intervals. It is not clear how much this IMF change will cause the change in the wavelength of mirror modes. For example, if the IMF simply changes to its opposite direction, the frequency of mirror waves may remain the same. Because the compressional waves in the middle and inner sheath have different frequencies, they are not the same wave due simply to convection effects. Furthermore, their modes are different. Because it is difficult to damp the mirror waves quickly while a new mode emerges, it is more natural that the slow wave occurs at a mode conversion of mirror modes. Because the slow wave is of observed frequencies lower than mirror modes, the wave propagates against the flow as indicated in the third expression of equation (7).

The waves in the outer magnetosheath (see Figure 5) are much weaker than that in the middle and inner sheath in the intermediate frequencies and are predominantly transverse over the full frequency range. The transverse ratio is large and the compressional ratio is small, indicating the waves are Alfvénic. The Alfvén Mach number is close to 1. The Alfvén ratio (see appendix A) is smaller than unity. The mirror waves in the middle sheath (Figure 4) appear to be additional wave power to the Alfvén-like waves in the outer sheath, indicating that the wave in the middle sheath is due to the growth of a new wave.

Nonlinear Effects

Our scheme is based on linear theory. Two of our four ratios depend on the dispersion relation. For waves of a finite amplitude, C. F. Kennel (unpublished manuscript, 1989) has shown that the dispersion relation for the three MHD modes remains the same as in linear theory but the values of background parameters are replaced by local values. A fluctuation of 10-20% in the background values will not change our criteria qualitatively. Therefore our scheme should be applicable to waves of a finite amplitude as shown in our test case. However, as will be discussed below, nonlinear effects may be important to explain the presence of the slow magnetosonic mode. In the magnetosheath downstream of quasi-parallel shocks, the amplitude of the magnetic field perturbations may be comparable to the average field [*Engebretson et al.*, 1991]. We will investigate these large-amplitude waves and report on them elsewhere.

A major difference between linear kinetic theory and linear MHD theory is that the former theory predicts strong Landau damping for quasi-perpendicular slow magnetosonic modes, whereas the latter theory does

not. The Landau damping arises from the wave resonating with the parallel motion of particles; as particles gain energy in this process, the wave is damped. However, the more complete description provided by kinetic theory is at the cost of stronger restriction in deriving its linear theory. There are three effects [e.g., *Barnes*, 1979] that counteract Landau damping. The Landau damping rate calculated from linear theory is based on the Maxwellian distribution of the particles. A non-Maxwellian distribution may result in a different damping rate. When the wave is of a finite amplitude, Landau damping needs to compete with the nonlinear steepening of the wave. Finally, the linearization of the kinetic theory breaks down when the Landau damping time is longer than the bounce time of a particle reflected within the magnetic cavity formed by the compressional wave [*Davidson*, 1972].

In order to get a quantitative feeling of the importance of the nonlinear effects, we use the estimate of the damping rate versus the nonlinear steepening rate provided by *Barnes* [1979],

$$t_d/t_s \sim 2\pi\ (\delta B/B)\ \exp(1/\beta)$$

where t_d and t_s are the damping time and steepening time. For Landau damping to occur, this ratio needs to be much smaller than unity and vice versa. For the waves we have identified as slow magnetosonic modes, $\delta B/B = 0.14$ and $\beta = 1.34$, the ratio is 1.9. Therefore the steepening is comparable to, if not stronger than, the damping. Similarly, we can also show that the bounce time for trapped particles is shorter than the damping time, i.e., the linearization of kinetic theory breaks down for the observed wave amplitude.

The physical meaning of the above estimate is clear. Although the nonlinear effects for an amplitude of 14% do not invalidate MHD linear theory, it is significant for linear kinetic theory. Therefore Landau damping of the slow magnetosonic wave [*Barnes*, 1966] in the inner magnetosheath could be suppressed by nonlinear effects. The mirror mode upstream may provide a finite amplitude for the slow magnetosonic mode, and thus the slow wave does not grow from the linear stage in kinetic theory. Here we should point out some of misunderstandings in interpreting the results of *Hada*

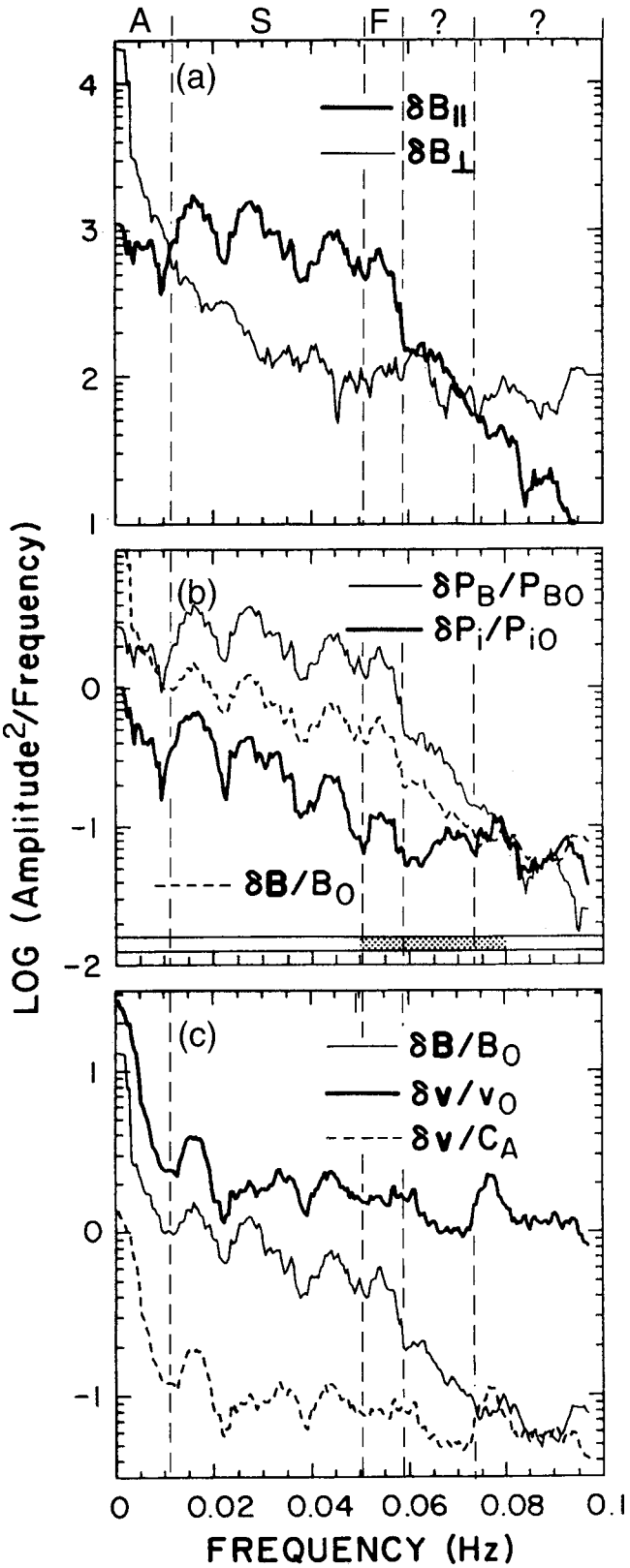

Figure 3. The Fourier spectra of the fluctuations in the inner magnetosheath. (a) The transverse, $(\delta\mathbf{B}\cdot\delta\mathbf{B} - \delta B_{\parallel}^2)/f$ (thin line), and compressional $\delta B_{\parallel}^2/f$ (thick line), powers of the magnetic field; (b) the magnetic pressure, $\delta P_B^2/P_{Bo}^2/f$ (thin solid line), thermal pressure, $\delta P_i^2/P_{io}^2/f$ (thick line) and magnetic field, $\delta\mathbf{B}\cdot\delta\mathbf{B}/B_0^2/f$ (dashed line); and (c) the magnetic field, $\delta\mathbf{B}\cdot\delta\mathbf{B}/B_0^2/f$ (thin solid line), velocity normalized by the average velocity, $\delta\mathbf{v}\cdot\delta\mathbf{v}/v_0^2/f$ (thick line), and velocity normalized by the Alfvén velocity, $\delta\mathbf{v}\cdot\delta\mathbf{v}/C_A^2/f$ (dashed line). The bar in the lower part of Figure 3b indicates the phase relation between the magnetic and thermal pressures: open bar for out of phase and shaded bar for in phase. The vertical dashed lines separate the frequencies of each identified mode as shown by the letter at the top of the figure. A, S, M, and F denote the Alfvén-like quasi-perpendicular slow magnetosonic, mirror, and fast magnetosonic mode, respectively. The question mark indicates classification of the waves is difficult.

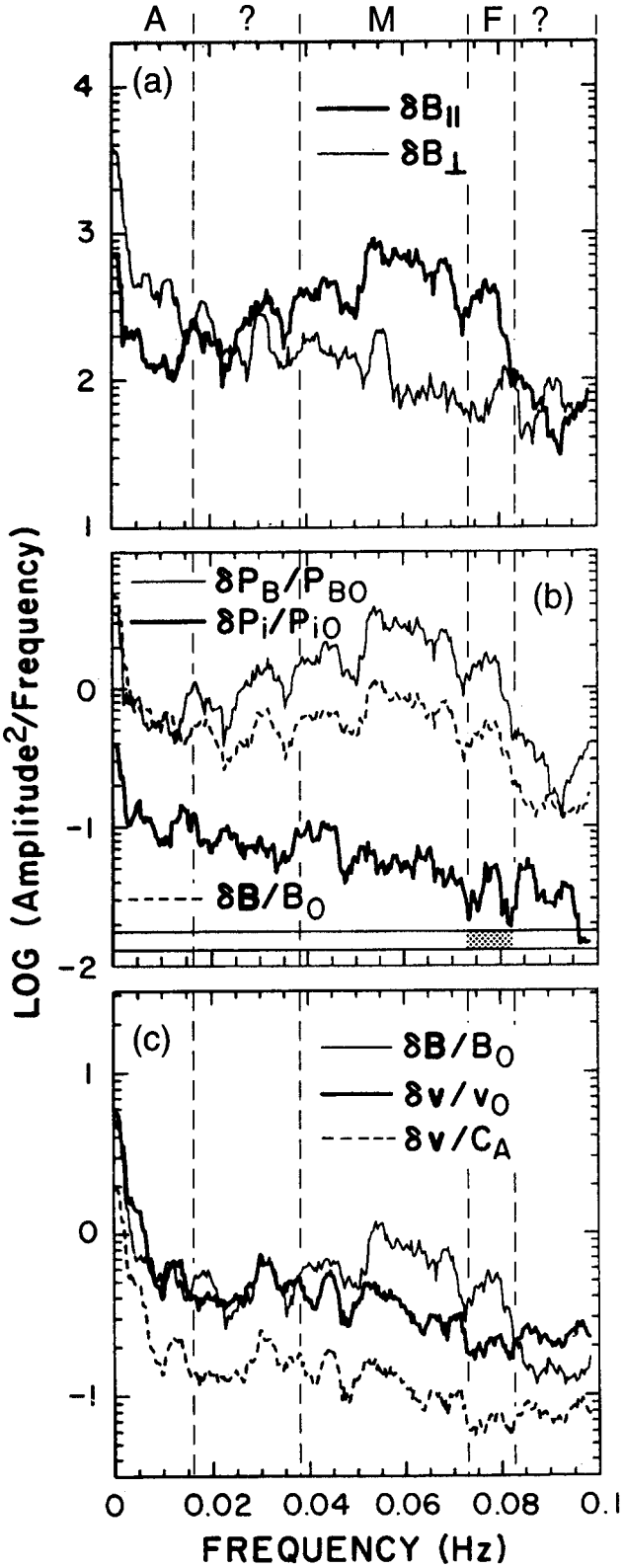

Figure 4. The Fourier spectra of the fluctuations in the middle of the magnetosheath in the same format as Figure 3. Note a major difference between these waves and those in Figure 3 is that the thin solid line is above the thick line in the frequencies from 0.05 to 0.08 Hz in Figure 4c (the Doppler ratio is less than 1) but not in Figure 3c, indicating the waves in Figure 3 are slow modes but those in Figure 4 are mirror modes.

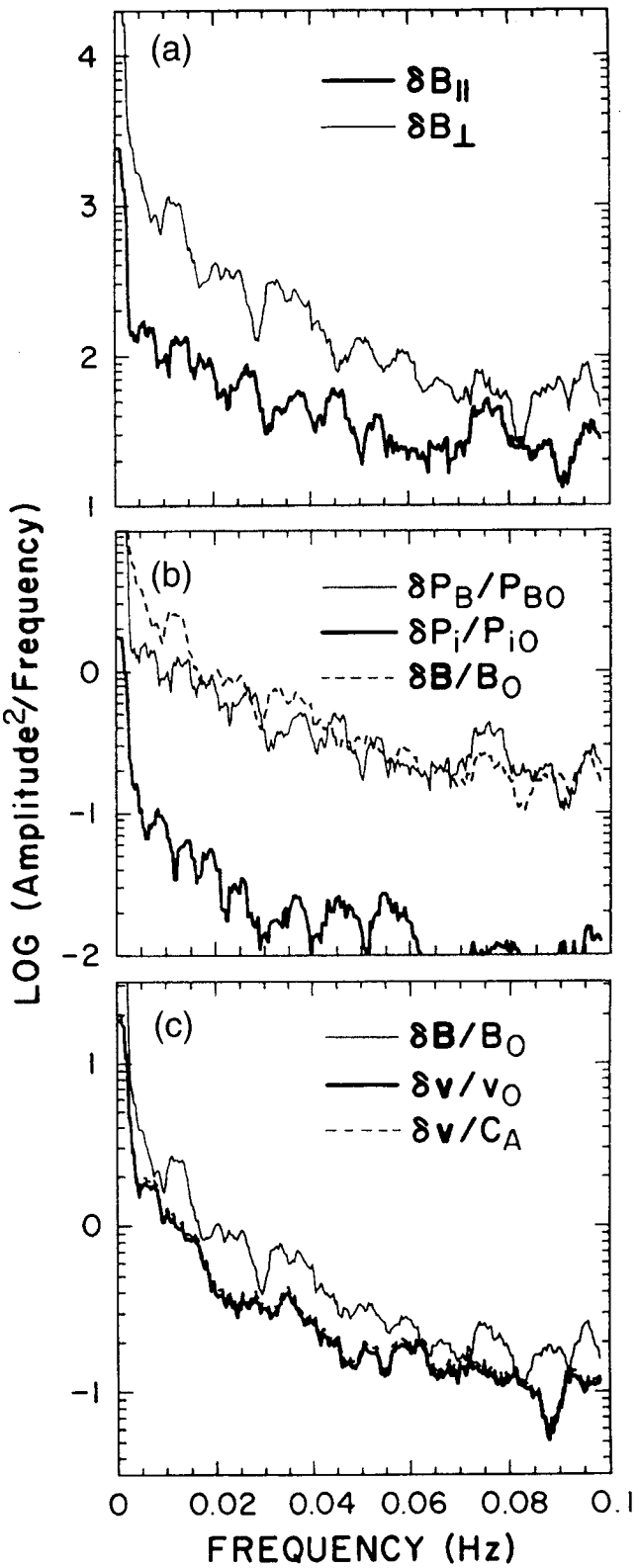

Figure 5. The Fourier spectra of the fluctuations in the outer magnetosheath in the same format as Figure 3. The phase relation in the Figure 5c is not shown. The whole frequency range has been identified as the Alfvén-like mode.

and Kennel [1985]. Many have used Figure 2 of Hada and Kennel as evidence for Landau damping of the slow magnetosonic mode. The wave amplitude in this calculation is only 1%. As shown in their Figure 5, under condition in the sheath, Landau damping is overcome by nonlinear steepening when the amplitude is greater than 10%.

Summary and Discussion

We have developed a scheme, illustrated in Figure 1, which uses measurements from a single spacecraft to determine the modes of low-frequency fluctuations. The uniqueness of the method is that the waves of different frequencies can be identified on the same spectra and that the Doppler shift can be resolved to some extent. The method does not rely on accurate intercalibration among instruments. The mode identification does not depend on the wave vector determination. Note here that different waves may not propagate in the same direction. The traditional wave vector determination method, the minimum variance technique for example, provides a wave vector for the component of the wave with the greatest power. Furthermore, the uncertainty of the wave vector determination is large for linearly polarized waves. In addition to this mode identification, further work is needed in order to determine the propagation direction for each mode.

We have applied our identification scheme to the analysis of fluctuation data from an AMPTE/IRM magnetosheath pass near the Sun-Earth line downstream of a quasi-perpendicular shock. The results show the evolution of the wave modes from the outer to inner magnetosheath. In the outer sheath near the bow shock, the full frequency range (10^{-3} Hz to 10^{-1} Hz) is dominated by transverse magnetic fluctuations; we identify these as Alfvén-like modes. In the middle magnetosheath, the fluctuations with the largest energy density are compressional at 0.02 Hz $< f <$ 0.07 Hz which we have identified as due to the mirror instability. Alfvén-like modes persist at lower frequencies. Closer to the magnetopause in the inner sheath, compressional fluctuations dominate the spectra at 0.01 Hz $< f <$ 0.05 Hz; we identify these as quasi-perpendicular slow magnetosonic, or mirrorlike, modes. Transverse Alfvén-like modes are most important at lower frequencies. Fast modes exist in the high-frequency end of the wave enhancements in the middle and inner magnetosheath.

We have shown that for a steady state magnetosheath, the measured frequency of a wave remains close to constant as the wave convects and propagates through the magnetosheath. Changes in the solar wind and IMF may affect the steady state condition. If a satellite orbit is significantly different from a steady state streamline and the wave properties change radically from one streamline to another, the frequency invariant does not apply. If this invariant is applicable to our test case, the mirror waves observed in the middle sheath are newly growing waves which do not exist in the outer sheath. These mirror waves may change to upstream propagating slow magnetosonic mode in the inner sheath. Nonlinear effects may be important for the slow magnetosonic mode waves to survive Landau damping. Using two spacecraft measurements, *Song et al.* [1992b] provide independent evidence for this possible evolution in the wave mode. Because the wave-particle interaction is weak for these low-frequency waves, the plasma conditions, such as β and the temperature anisotropy, may not change significantly in the mode conversion. Thus the region with the slow magnetosonic mode remains the condition marginally stable to the mirror mode.

Appendix A

Compressional ratio. The dispersion relation and perturbations for the two MHD compressional modes are

$$v_{ph}^2 = \frac{1}{2}\left\{(c_s^2 + C_A^2) \pm \left[(c_s^2 + C_A^2)^2 - 4c_s^2\, C_A^2\, \cos^2\theta\right]^{1/2}\right. \tag{A1}$$

$$\frac{\delta P_i}{P_{io}} = \left[1 - \frac{c_s^2\, \cos^2\theta}{v_{ph}^2}\right]^{-1} \frac{\gamma \delta B_{||}}{B_0} \tag{A2}$$

where $\delta P_i, P_{io}, \delta B_{||}$ and B_0 are the perturbed and background thermal pressure and field strength; γ is the polytropic index; θ is the angle between the wave vector and background field; and v_{ph}, c_s, and C_A are the phase speed of the wave, the sound speed, and the Alfvén speed. The plus and minus signs are for fast and slow modes, respectively. For nearly parallel propagation waves, $\cos\theta \sim 1$, in a high-β plasma, $c_s > C_A$, we have

$$v_{ph}^2 = \frac{1}{2}\left[c_s^2 + C_A^2 \pm \left(c_s^2 - C_A^2 + \frac{2c_s^2 C_A^2 \sin^2\theta}{c_s^2 - C_A^2}\right)\right] \tag{A3a}$$

This is, for the fast mode,

$$v_{phf}^2 = c_s^2\left[1 + C_A^2 \sin^2\theta/(c_s^2 - C_A^2)\right] \tag{A3b}$$

and for the slow mode,

$$v_{phs}^2 = C_A^2\left[1 - c_s^2 \sin^2\theta/(c_s^2 - C_A^2)\right] \tag{A3c}$$

Note

$$\delta B_{||} = \delta B_z = -\delta B_x \tan\theta \tag{A4}$$

where δB_x is the transverse component of the perturbation which lies on the coplanar plane and the background field is B_z. Combining equations (A2), (A3), and (A4) for the fast mode, we have

$$\frac{\delta P_i}{P_{io}} = -\frac{c_s^2 - C_A^2\cos^2\theta}{c_s^2\, \sin\theta\cos\theta}\,\gamma\frac{\delta B_x}{B_0} \tag{A5a}$$

and for the slow mode,

$$\frac{\delta P_i}{P_{io}} = \tan\theta \frac{\gamma C_A^2(c_s^2 \cos^2\theta - C_A^2)}{c_s^4 \cos^2\theta + C_A^4 - 2C_A^2 c_s^2 \cos^2\theta} \frac{\delta B_x}{B_0} \quad \text{(A5b)}$$

From equation (A5) when $\theta \to 0$, the compressional ratio, $(\delta P_i^2/P_{io}^2)/(\delta\mathbf{B}\cdot\delta\mathbf{B}/B_0^2)$, goes to infinity for the fast mode and zero for the slow mode.

Similarly, for nearly perpendicular propagation waves, we have

$$v_{phf}^2 = c_s^2 + C_A^2 - \frac{c_s^2 C_A^2 \cos^2\theta}{c_s^2 + C_A^2} \quad \text{(A6a)}$$

$$v_{phs}^2 = \frac{c_s^2 C_A^2 \cos^2\theta}{c_s^2 + C_A^2} \quad \text{(A6b)}$$

The perturbation relation for the fast mode is

$$\frac{\delta P_i}{P_{io}} = \frac{(c_s^2 + C_A^2)^2 - c_s^2 C_A^2 \cos^2\theta}{(c_s^2 + C_A^2)^2 - c_s^2 \cos^2\theta\,(2C_A^2 + c_s^2)} \frac{\gamma \delta B_{||}}{B_0} \quad \text{(A7a)}$$

and for the slow mode,

$$\frac{\delta P_i}{P_{io}} = -\gamma \frac{C_A^2}{c_s^2} \frac{\delta B_{||}}{B_0} \quad \text{(A7b)}$$

Note that $\delta B_x \ll \delta B_{||}$ when $\theta \to \pi/2$. The compressional ratio is $4/\beta^2$ for the slow mode and γ^2 for the fast mode. This ratio is not very useful in distinguishing the two modes for quasi-perpendicular propagation because the ratio is similar if β remains finite. The compressional ratio is physically similar to, with a factor of γ^2 difference, the compressibility of *Gary* [1986] and *Gary and Winske* [1992]. We choose to use the thermal pressure rather than the density, because it is less sensitive to thermal noise.

Doppler ratio. Under the frozen-in assumption, in the Earth's frame Faraday's law is

$$(\mathbf{B}\cdot\nabla)\mathbf{v} - (\mathbf{v}\cdot\nabla)\mathbf{B} - \mathbf{B}\cdot(\nabla\cdot\mathbf{v}) = \frac{\partial \mathbf{B}}{\partial t} \quad \text{(A8)}$$

The right-hand term depends on the frame. For example, for the mirror instability in the saturated stage, this term is zero in the plasma frame, but not zero in the spacecraft frame. The linear perturbations in the spacecraft frame are

$$\mathbf{B}_0(\mathbf{k}\cdot\delta\mathbf{v}) - (\mathbf{B}_0\cdot\mathbf{k})\delta\mathbf{v} = \omega\delta\mathbf{B} \quad \text{(A9)}$$

where $\omega = \omega' - \mathbf{k}\cdot\mathbf{v}_0$ is the frequency in the plasma frame and ω' is the frequency measured in the Earth's frame. For the Alfvén mode, $\mathbf{k}\perp\delta\mathbf{v}$, the first term on the left-hand side of equation (A9) is zero. Since $v_{ph} = C_A\cos\theta$, we have

$$\pm\frac{\delta\mathbf{v}}{C_A} = \frac{\delta\mathbf{B}}{B_0} \quad \text{(A10)}$$

Thus $(\delta\mathbf{v}/C_A)/(\delta\mathbf{B}/B_0)$, the Alfvén ratio [*Matthaeus and Goldstein*, 1982a; *Gary and Winske*, 1992], is close to ±1 for the Alfvén mode. The minus and plus signs represent the waves propagating parallel and antiparallel to the field, respectively. The Alfvén ratio is plotted in Figures 3c, 4c, and 5c. There is a significant discrepancy between observation and linear theory [*Belcher et al.*, 1969; *Matthaeus and Goldstein*, 1982a, b; *Roberts et al.*, 1987, 1990]. Usually, the observed Alfvén ratio in the solar wind is about half of that from theory. Under the magnetosheath condition, linear theory predicts the Alfvén ratio to be greater than 1 for both fast and slow modes, near 1 for the Alfvén mode, and much smaller for the mirror mode. However, as shown in Figures 3c, 4c, and 5c, the Alfvén ratio is significantly smaller than unity through most frequencies in all regions. It is impossible for all these waves to be the mirror mode because some of them are transverse.

For the two compressional modes, we have, from the continuity equation,

$$\mathbf{k}\cdot\delta\mathbf{v} = \omega\frac{\delta B_{||}}{B_0}\frac{v_{ph}^2}{v_{ph}^2 - c_s^2\cos^2\theta} \quad \text{(A11)}$$

Here we have used the perturbation relations for the two compressional modes, equation (A2) and

$$\frac{\delta P_i}{P_{io}} = \gamma\frac{\delta\rho}{\rho_0} \quad \text{(A12)}$$

where $\delta\rho$ and ρ_0 are the perturbed and average densities. From equations (A9) and (A11), we have

$$\cos\theta\frac{\delta\mathbf{v}}{v_{ph}} = -\frac{\delta\mathbf{B}}{B_0} + \frac{\mathbf{B}_0\delta B_{||}}{B_0^2}\left(\frac{v_{ph}^2}{v_{ph}^2 - c_s^2\cos^2\theta}\right) \quad \text{(A13)}$$

For nearly perpendicular propagating slow mode waves in a high-β plasma,

$$\frac{\delta v}{C_A} = -\frac{\delta B}{B_0}\left(1 + \frac{2}{\gamma\beta}\right)^{1/2}$$

The Doppler ratio is $[1 + (2/\gamma\beta)]/M_A^2$, where $M_A = v_0/C_A$ is the Alfvén Mach number. When the flow velocity is comparable to or smaller than the Alfvén velocity, the Doppler ratio, $(\delta\mathbf{v}\cdot\delta\mathbf{v}/v_0^2)/(\delta\mathbf{B}\cdot\delta\mathbf{B}/B_0^2)$, is greater than unity.

Since the mirror mode with the greatest growth rate is nearly perpendicular to the background magnetic field, from equation (A9), we have

$$\mathbf{k}\cdot\delta\mathbf{v} = \frac{\mathbf{B}_0\cdot\delta\mathbf{B}}{B_0^2}\omega \quad \text{(A14)}$$

Note $\omega' - \omega = \mathbf{k}\cdot\mathbf{v}$. Therefore the Doppler ratio $(\delta\mathbf{v}\cdot\delta\mathbf{v}/v_0^2)/(\delta\mathbf{B}\cdot\delta\mathbf{B}/B_0^2)$ is of the order of $[\omega/(\omega'-\omega)]^2$, the reason why the parameter is so named. For the mirror mode $\omega \ll \omega'$, the ratio is much smaller than unity. In the growth stage of the mirror mode, the growth rate should also be included in ω^2. Kinetic theory has shown that under typical sheath conditions, the maximum growth rate of the mirror mode is less than $10^{-2}f_{ci}$, where f_{ci} is the ion gyrofrequency [*Gary*, 1992]. The observed mirror mode waves are of Doppler-shifted

frequencies greater than 0.1 f_{ci}. Therefore the above criterion is also justified in the growth phase of the mirror mode. In the saturated stage of the mirror mode, ω is small. One may consider dropping the right-hand term in evaluation of equation (A9). Because $\delta \mathbf{v} = i\omega\xi$, where ξ is the displacement associated with the instability, $\delta \mathbf{v}$ is also very small.

Appendix B

This paper has described a procedure for identifying low-frequency magnetic fluctuations observed in space plasmas. The purpose of this appendix is to compare this procedure with the somewhat different approach discussed by *Gary and Winske* [1992] (Hereafter GW) and *Gary* [1992].

There are three fundamental differences between the present procedure and that of GW. The present scheme is based upon linear MHD theory, utilizes four identifiers (Transverse ratio, compressional ratio, partition ratio, and Doppler ratio), and involves a "tree-root" procedure. The GW procedure utilizes linear Vlasov theory, involves six identifiers (Damping/growth rate, helicity, cross-helicity, compressibility, parallel compressibility, and Alfvén ratio), and is based upon a parallel procedure, or an identification matrix.

If the plasma of concern is relatively isotropic, linear MHD theory and linear Vlasov theory in the long wavelength, low frequency limit should yield equivalent results for identifiers if the mode of concern is weakly damped. For a heavily damped mode, the identifiers may be somewhat different, but in this case Vlasov theory rejects this mode because of the damping. Because GW found that the obliquely propagating slow mode is heavily damped for magnetosheath conditions, they do not consider it a mode likely to be observed in the regions farther than a wavelength from the source which may be the magnetopause. This paper has argued that finite amplitude effects can overwhelm Landau damping and permit slow modes to propagate in the sheath.

The helicity and cross-helicity identifiers used by GW and *Gary* [1992] may be convenient for the extremely long wavelength, low frequency fluctuations observed in the solar wind, but are less convenient for identifying magnetic fluctuations up to the proton cyclotron frequency observed in the magnetosheath and magnetosphere. For the latter type of fluctuations, identifiers such as the transverse ratio of this paper, which directly utilize the information available in spacecraft observations of the magnetic field vector, are much more useful in determining mode identity. On the other hand, for modest amplitude fluctuations for which nonlinear effects are weak, the damping/growth rate of linear Vlasov theory can provide useful additional information. This is particularly important for plasmas which are sufficiently anisotropic such that instabilities can be excited. When observations of plasma distribution functions are available, an optimum set of identifiers might consist of four quantities similar to those used in this paper plus the damping/growth rate for each mode. If the fluctuations are of relatively large amplitude, the latter quantity should be determined from nonlinear theories and computer simulations [eg., *McKean et al.*, 1992; *Omidi et al.*, 1994].

The "tree-root" procedure of this paper successively eliminates candidate modes through a sequence of Yes or No identifications. However, if one uses the "parallel" procedure and the six identifiers described by GW, the two procedures can yield different results in some cases. The following discussion shows such an example.

The fluctuations between 0.01 and 0.05 Hz in Figure 3 have been identified as obliquely propagating slow modes in Section 4 of this paper. Application of the identification matrix yields a different conclusion. The observed fluctuations correspond to the following values of five identifiers: GW compressibility $\ll 1$; GW parallel compressibility < 0; GW Alfvén ratio $\ll 1$; Transverse ratio $\ll 1$; Damping/growth rate should be small because the waves exist in a large region with a similar amplitude.

The theoretical predictions of the formalism described by *Gary* [1992] are that fluctuations due to the mirror instability satisfy all five of these criteria, under the assumption that the proton temperature anisotropy is sufficiently large to avoid damping of this mode. The theory of GW predicts that the obliquely propagating slow mode has a negative parallel compressibility and a small transverse ratio, in agreement with observations. But GW also predicts that the slow mode should have a compressibility much larger than unity, an Alfvén ratio much larger than unity, and, for the $T_e \ll T_p$ condition of the magnetosheath, a strongly negative damping rate (The presence of a temperature anisotropy large enough to excite the mirror instability does not significantly reduce this damping). Thus the GW procedure would identify these fluctuations as associated with the mirror instability.

In summary, the differences between two sets of identifiers and procedures may result in ambiguity in the mode identifications. In order to resolve the ambiguity, further investigations from nonlinear kinetic theory, simulation and observation are crucial.

Acknowledgments. We wish to thank A. Richmond for valuable discussions. Helpful discussions with D. G. Sibeck, R. J. Strangeway, and T. Bogdan are gratefully acknowledged. The work at UCLA was supported by a research grant from the National Science Foundation, ATM91-11913, and a grant from the IGPP Branch at Los Alamos. The LANL portion of this work was performed under the auspices of the U.S. Department of Energy (DOE) and was supported by the DOE Office of Basic Energy Sciences, Division of Engineering and Geosciences, and the Space Plasma Theory Program of the National Aeronautics and Space Administration (NASA). One of us (P.S.) would like to thank E. Zweibel for careful reading of the draft of the paper and many useful comments and suggestions, and thank Liz Boyd for her assistance in preparing this manuscript. The National Center for Atmospheric Research is sponsored by the National Science Foundation. The NSSDC provided the data from AMPTE/IRM (PIs, H. Luehr for triaxial flux gate data and G. Paschmann for 3-D plasma data).

The Editor thanks N. Lin and another referee for their assistance in evaluating this paper.

References

Anderson, B. J., S. A. Fuselier, and D. Murr, Electromagnetic ion cyclotron waves observed in the plasma depletion layer, *Geophys. Res. Lett., 18*, 1955, 1991.

Anderson, B. J., S. A. Fuselier, S. P. Gary, and R. E. Denton, Magnetic spectral signatures in the Earth's magnetosheath and plasma depletion layer, *J. Geophys. Res.*, in press, 1994.

Barnes, A., Collisionless damping of hydromagnetic waves, *Phys. Fluids, 9*, 1483, 1966.

Barnes, A., Hydromagnetic waves and turbulence in the solar wind, in *Solar System Plasma Physics*, edited by E. N. Parker, C. F. Kennel, and L. J. Lanzerotti, pp. 249-319, North-Holland, New York, 1979.

Barnes, A., Theory of magnetohydrodynamic waves: The WKB approximation revisited, *J. Geophys. Res., 97*, 12,105, 1992.

Belcher, J. W., L. Davis, and E. J. Smith, Large-amplitude Alfvén waves in the interplanetary medium: Mariner 5, *J. Geophys. Res., 74*, 2302, 1969.

Brinca, A. L., N. Sckopke, and G. Paschmann, Wave excitation downstream of the low-β, quasi-perpendicular bow shock, *J. Geophys. Res., 95*, 6331, 1990.

Cummings, W. D., and P. J. Coleman, Jr., Magnetic fields in the magnetopause and vicinity at synchronous altitude, *J. Geophys. Res., 73*, 5699, 1968.

Davidson, R. C., *Methods in Nonlinear Evolution Plasma Theory*, Academic, San Diego, Calif., 1972.

Dewar, R. L., Interaction between hydromagnetic waves and a time-dependent, inhomogeneous medium, *Phys. Fluids, 13*, 2710, 1970.

Engebretson, M. J., N. Lin, W. Baumjohann, W. Luehr, B. J. Anderson, L. J. Zanetti, T. A. Potemra, R. L. McPherron, and M. G. Kivelson, A comparison of ULF fluctuations in the solar wind, magnetosheath, and dayside magnetosphere, 1, Magnetosheath morphology, *J. Geophys. Res., 96*, 3441, 1991.

Fairfield, D. H., Waves in the vicinity of the magnetopause, in *Magnetospheric Particles and Field*, edited by B. M. McCormac, 333 pp., D. Reidel, Dordrecht, Netherlands, 1976.

Gary, S. P., Low-frequency waves in a high-β collisionless plasma: Polarization, compressibility and helicity, *J. Plasma Phys., 35*, 431, 1986.

Gary, S. P., The mirror and ion cyclotron anisotropy instabilities, *J. Geophys. Res., 97*, 8519, 1992.

Gary, S. P., and D. Winske, Correlation function ratios and the identification of space plasma instabilities, *J. Geophys. Res., 97*, 3103, 1992.

Gary, S. P., S. A Fuselier, and B. J. Anderson, Ion anisotropy instabilities in the magnetosheath, *J. Geophys. Res., 98*, 1481, 1993.

Gleaves, D. G., and D. J. Southwood, Magnetohydrodynamic fluctuations in the Earth's magnetosheath at 1500 LT: ISEE 1 and ISEE 2, *J. Geophys. Res., 86*, 129, 1991.

Hada, T., and C. F. Kennel, Nonlinear evolution of slow waves in the solar wind, *J. Geophys. Res., 90*, 531, 1985.

Hasegawa, A., *Plasma Instabilities and Nonlinear Effects*, 241 pp., Springer-Verlag, New York, 1975.

Hubert, D., Nature and origin of wave modes in the dayside earth magnetosheath, *Adv. Space Res.*, in press, 1994.

Hubert, D., C. Perche, C. C. Harvey, C. Lacombe, and C. T. Russell, Observation of mirror waves downstream of a quasi-perpendicular shock, *Geophys. Res. Lett., 16*, 159, 1989a.

Hubert, D., C. C. Harvey, and C. T. Russell, Observations of magnetohydrodynamic modes in the Earth's magnetosheath at 0600 LT, *J. Geophys. Res., 94*, 17,305, 1989b.

Kaufmann, R. L., J.-T. Horng, and A. Wolfe, Large-amplitude hydromagnetic waves in the inner magnetosheath, *J. Geophys. Res., 75*, 4666, 1970.

Krauss-Varban, D., N. Omidi, and K. B. Quest, Mode properties of low-frequency waves: Kinetic theory versus Hall-MHD, *J. Geophys. Res.*, in press, 1994.

Lacombe, C., F. G. E. Pantellini, D. Hubert, C. C. Harvey, A. Mangeney, G. Belmont, and C. T. Russell, Mirror and Alfvénic waves observed by ISEE 1-2 during crossings of the Earth's bow shock, *Ann. Geophys., 10*, 772, 1992.

Lee, L. C., C. P. Price, and C. S. Wu, A study of mirror waves generated downstream of a quasi-perpendicular shock, *J. Geophys. Res., 93*, 247, 1988.

Lee, L. C., M. Yan, and J. G. Hawkins, A study of slow mode structure in front of the dayside magnetopause, *Geophys. Res. Lett., 18*, 381, 1991.

Lin, N., M. J. Engebretson, R. L. McPherron, M. G. Kivelson, W. Baumjohann, M. Luehr, T. A. Potemra, B. J. Anderson, and L. J. Zanetti, A comparison of ULF fluctuations in the solar wind, magnetosheath, and dayside magnetosphere, 2, Field and plasma conditions in the magnetosheath, *J. Geophys. Res., 96*, 3455, 1991a.

Lin, N., M. J. Engebretson, W. Baumjohann, and H. Luhr, Propagation of perturbation energy fluxes in the subsolar magnetosheath: AMPTE IRM observations, *Geophys. Res. Letts., 18*, 1667, 1991b.

Matthaeus, W. H., and M. L. Goldstein, Measurements of the rugged invariants of magnetohydrodynamic turbulence in the solar wind, *J. Geophys. Res., 87*, 6011, 1982a.

Matthaeus, W. H., and M. L. Goldstein, Stationarity of magnetohydrodynamic fluctuations in the solar wind, *J. Geophys. Res., 87*, 10,347, 1982b.

McKean, M. E., D. Winske, and S. P. Gary, Kinetic properties of mirror waves in magnetosheath plasmas, *Geophys. Res. Lett., 19*, 1331, 1992.

Neugebauer, M., C. T. Russell, and E. J. Smith, Observations of the internal structure of the magnetopause, *J. Geophys. Res., 78*, 499, 1974.

Omidi, N., and D. Winske, Slow waves as part of the magnetopause structure, *Eos Trans. AGU, 73*, 459, 1992.

Omidi, N., A. O'Farrell, and D. Krauss-Varban, Sources of magnetosheath waves and turbulence, *Adv. Space Res.*, in press, 1994.

Price, C. P., D. W. Swift, and L.-C. Lee, Numerical simulation of nonoscillatory mirror waves at the Earth's magnetosheath, *J. Geophys. Res., 91*, 101, 1986.

Rezeau, L., A. Morane, S. Perraut, A. Roux, and R. Schmidt, Characterization of Alfvénic fluctuations in the magnetopause boundary layer, *J. Geophys. Res., 94*, 101, 1989.

Roberts, D. A., L. W. Klein, M. L. Goldstein, and W. H. Matthaeus, The nature evolution of magnetohydrodynamic fluctuations in the solar wind: Voyager observations, *J. Geophys. Res., 92*, 11021, 1987.

Roberts, D. A., M. L. Goldstein, and L. W. Klein, The amplitude of interplanetary fluctuations: Stream structure, heliocentric distance, and frequency dependence, *J. Geophys. Res., 95*, 4203, 1990.

Russell, C. T., W. Riedler, K. Schwingenschuh, and Y. Yeroshenko, Mirror instability in the magnetosphere of comet Halley, *Geophys. Res. Lett., 14*, 644, 1987.

Sckopke, N., G. Paschmann, A. L. Brinca, C. W. Carlson, and H. Luhr, Ion thermalization in quasi-perpendicular shocks involving reflected ions, *J. Geophys. Res., 95*, 6337, 1990.

Song, P., R. C. Elphic, C. T. Russell, J. T. Gosling, and C. A. Cattell, Structure and properties of the subsolar magnetopause for northward IMF: ISEE observations, *J. Geophys. Res., 95*, 6375, 1990a.

Song, P., C. T. Russell, J. T. Gosling, M. F. Thomsen, and

R. C. Elphic, Observations of the density profile in the magnetosheath near the stagnation streamline, *Geophys. Res. Lett., 17*, 2035, 1990b.

Song, P., C. T. Russell, and M. F. Thomsen, Slow mode transition in the frontside magnetosheath, *J. Geophys. Res., 97*, 8295, 1992a.

Song, P., C. T. Russell, and M. F. Thomsen, Waves in the inner magnetosheath: A case study, *Geophys. Res. Lett., 9*, 2191, 1992b.

Song, P., C. T. Russell, and C. Y. Huang, Wave properties near the subsolar magnetopause: Pc 1 waves in the sheath transition layer, *J. Geophys. Res., 98*, 5907, 1993.

Southwood, D. J., and M. G. Kivelson, On the form of the flow in the magnetosheath, *J. Geophys. Res., 97*, 2873, 1992.

Southwood, D. J., and M. G. Kivelson, Mirror instability, 1, The physical mechanism of linear instability, *J. Geophys. Res., 98* 9181, 1993.

Takahashi, K., D. G. Sibeck, P. T. Newell, and H. E. Spence, ULF waves in the low-latitude boundary layer and their relationship to magnetospheric pulsation: A multisatellite observation, *J. Geophys. Res., 96*, 9503, 1991.

Tsurutani, B. T., E. J. Smith, R. R. Anderson, K. W. Ogilvie, J. D. Scudder, D. N. Baker, and S. J. Bame, Lion roars and nonoscillatory drift mirror waves in the magnetosheath, *J. Geophys. Res., 87*, 6060, 1982.

S. P. Gary, Los Alamos National Laboratory, Los Alamos, NM 87545. (e-mail:Internet.pgary@sstcx1.lanl.gov)

C. T. Russell, Institute of Geophysics and Planetary Physics, University of California, Los Angeles, CA 90024. (e-mail:Internet.ctrussell@igpp.ucla.edu)

P. Song, High Altitude Observatory, National Center for Atmospheric Research, P.O. Box 3000, Boulder, CO 80307. (e-mail:Internet.psong@hao.ucar.edu)

(Received June 16, 1993; revised October 25, 1993; accepted November 11, 1993.)